ELECTROSTATIC PRECIPITATORS

Electrostatic precipitation is the removal of solid or liquid particulate matter from a gas stream with electrical forces. The process consists of particle charging, transport to a collecting surface, deposition on that surface, and ultimately, removal from the collection surface. In a modern precipitator, these steps can be separate processes or can take place simultaneously, depending on the design and operation of the equipment.

Electrostatic precipitation has a number of distinguishing features that make it suitable for a broad range of applications. Most electrostatic precipitators are simple devices with few moving parts. This simplicity makes cleaning of very dirty gas streams possible, and, with the use of corrosion resistant materials, even corrosive gas streams can be cleaned. The pressure drop through a precipitator is very low, making possible the cleaning of large volumes of gas economically. The electrical power consumed is likewise small for the volume of gas treated. Finally, it is possible to achieve very high removal efficiencies in a compact system. The configuration of the equipment and the effects of particle and gas properties on the removal process are discussed in detail in the following sections.

Particle Separation Process

Particle Properties. It is useful to begin with a discussion of the properties of particles typically collected in electrostatic precipitators. Precipitators are well-suited for collecting particles of the sizes commonly generated by many industrial processes. These particles have effective diameters from less than 0.1 μm to over 200 μm. Particles larger than 200 μm settle so rapidly that they will fall out of the gas, unless its velocity is quite high. The term "effective diameter" is used because particles are not always spherical in shape. Precipitators readily collect irregular particles, but the theoretical treatment of the collection process always assumes spherical particles to simplify calculations.

Other particle properties that affect the separation process are the physical state (solid or liquid), the electrical resistivity, and the dielectric constant of insulating materials. Solid and liquid particles behave similarly in the gas stream, but quite differently when they reach the collection plate. The resistivity and dielectric constant have some effect on the charging rate of particles but resistivity plays its major role with the collected particles. In most precipitators, the collected particle on the surface form a dust layer through which electrical current must flow. If the resistivity of this layer is high, an electrical breakdown in the layer can occur, resulting in sparking or a phenomenon called back corona. In either case, the useful electrical power for precipitation is limited.

Corona. An electric corona is the key feature of operation of an electrostatic precipitator because it supplies the ions that charge the particles for subsequent collection. The corona discharge (see ELECTROSTATIC DISCHARGE) is created by the application of high voltage to a wire or electrode with sharp edges opposite a grounded plate. As illustrated in Fig. 1, the discharge electrode, shown as three vertical wires, has a small radius of curvature and the collecting surface, a large radius of curvature. This geometry produces a nonuniform electric field (see ELECTRIC FIELD MEASUREMENT) around the wire that is strongest at the surface of the wire. In any gas, there are always a few electrons and ions liberated by cosmic rays or radioactivity. In the vicinity of the discharge electrode, these naturally occurring electrons are accelerated by the intense electric field and gain enough energy to ionize more molecules. The ions generated by the corona process are responsible for charging particles. This process is discussed in more detail later.

The charging process is divided into two regimes for discussion: field charging and diffusion charging. Field charging results from the strong polarization of a particle in the electric field that draws ions toward the particle's surface. Diffusion charging results from the random collection of ions that strike the surface by chance. Generally speaking, field charging in a precipitator is the dominant mechanism for particles with diameters greater than 10 μm, while diffusion charging dominates for particles with diameters below 1 μm. For intermediate particle diameters, both mechanisms are important.

Under typical precipitator conditions, field charging is a rapid process, giving 80% of the maximum possible charge within a fraction of a second. Diffusion charging is slower, but continues to increase a particle's charge throughout its residence in the precipitator. The charging process is described in more detail later.

Electric Force on Particles

The electric fields in the precipitator provide the moving force that drives particles to the collecting surface. However, the trajectories of particles are far from simple because of the effects of turbulence (1). The flow in precipitators is turbulent because the flow rate must be kept high to treat the gas economically—lower flow rates require larger precipitators. At typical precipitator velocities, the flow is considered mildly turbulent with a quiet region near the collecting surfaces. In the turbulent part of the flow, the gas motion dominates the particle motion, but near the collecting surfaces, the electric field can drive the particles to the collecting surface at a predictable velocity. Since the charge on particles depends strongly on their diameters, the velocities near the surface vary considerably with size.

Collection. The nature of particle motion leads to the concept of a *migration velocity* that has been used to characterize the performance of electrostatic precipitators for many years. Although it is a quantity with the units of velocity, it represents an average collection rate that incorporates many effects not related to velocity. Later in this article, the equations needed to calculate the charge on particles and the electric fields in precipitators are presented. These equations make it possible to calculate with useful accuracy the electric forces on particles as they move through a precipitator and, ultimately, the overall collection performance. Still, the mi-

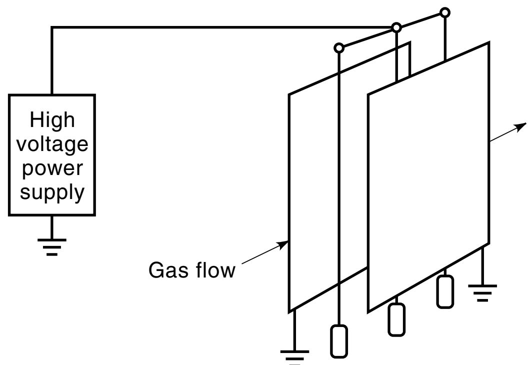

Figure 1. Principle of electrostatic precipitator operation: particle-laden gas flows past corona wires at high voltage for charging and collection.

gration velocity describes some of the performance aspects of precipitators quite well.

Collection Equations. To derive the classic form of the efficiency equation for precipitators, the collection process is assumed to consist of the removal of small numbers of particles from a uniformly mixed gas stream along each increment of length in the precipitator. Turbulence is assumed to keep the core of the flow mixed, and electric forces are responsible for removing the particles near the collecting surfaces. Moreover, the number removed is assumed to be proportional to the concentration of particles in the channel at any point. These assumptions lead to an exponential relationship:

$$\rho(x) = \rho(0)\exp(-cx) \tag{1}$$

where $\rho(x)$ is the particle concentration at distance x into the precipitator, and c is a collection rate parameter. This equation is more commonly written as:

$$eff = 100 \times \left[1 - \exp\left(-\frac{\omega A}{V}\right)\right] \tag{2}$$

where eff is the percentage collection efficiency, ω is the migration velocity, A is the plate area of the precipitator, and V is the gas volume treated. This is known as the Deutsch equation, after Walter Deutsch who first derived it (2, p 164). The assumption that collection is proportional to the local particle concentration is valid if particles are uniformly mixed in the gas, a reasonable assumption when measured at scales comparable to the distance between electrodes. At smaller scales, uniform mixing may not be maintained. Moreover, the collection rate parameter (c or ω) is expected to vary with particle size and charge.

The quantity A/V is known as the specific collection area (SCA); it indicates the size of the precipitator relative to the amount of gas it treats. The ratio of gas volume to plate area has the dimensions of velocity (3, p. 96), and we define it to be the specific precipitator velocity, ω_p:

$$\omega_p = \frac{V}{A} \tag{3}$$

The specific precipitator velocity can range from 0.7–10 cm/s, as shown in Table 1. The Deutsch equation can then be written in terms of the ratio of the migration velocity to the specific precipitator velocity, so that it becomes clear that the migration velocity needs to be 4 to 5 times as large as the specific precipitator velocity for high efficiency collection. Specific collector area is more commonly used for describing overall precipitator performance, while the specific precipitator velocity is useful in comparisons with velocities of particles of a specific size.

A modified Deutsch equation, called the Matts-Ohnfeldt equation (4), was derived to account for the range of particle sizes, but has also been shown to represent other effects, as well:

$$eff = 100 \times [1 - \exp(-(\omega_k/\omega_p)^k] \tag{4}$$

where k is a parameter, typically 0.4 to 0.6. The parameter ω_k is much larger than the parameter ω for the same precipitator. Although the form of the Matts–Ohnfeldt equation may seem strange, it matches the performance of operating precip-

Table 1. Examples of Precipitators

Type	Plate Area (m^2)	Gas Volume (m^3/s)	Voltage (kV)	Current (A)	Mass Efficiency (%)	Specific Precipitator Velocity, ω_p(cm/s)
Home Furnace	0.37	0.03	5	2.4×10^{-4}	95	8.1
Industrial Air Cleaner	2.5	0.10	12	1.0×10^{-3}	97	4.0
Two-stage Pilot Unit	13	0.025	50–45	4.6×10^{-4}	98.3	0.19
Industrial Boiler	2,300	41	30–20	0.03–0.12	91	1.8
Utility Boiler	5,900	117	54–48	0.32–0.68	99.92	2.0
Utility Boiler	7,800	288	51–40	0.60–0.80	98	3.7
Paper Mill	14,000	127	44–53	0.37–1.14	99.94	0.91
Utility Boiler	14,000	144	47–39	0.60–0.81	99.98	1.0
Utility Boiler	29,000	460	29–27	1.4–3.3	99.85	1.6
Utility Boiler	37,000	338	39–37	0.45–0.98	99.85[a]	0.91
Utility Boiler	41,000	630	37–40	0.60–0.80	99.92	1.5
Utility Boiler	86,000	584	43–32	1.0–2.8	99.76[a]	0.68
Utility Boiler	150,000	972	39–29	0.55–6.6	99.47[a]	0.65

[a] These precipitators experience a degrading condition known as back corona, but still achieve high efficiencies, primarily at the cost of extra size.
Voltage and current values are given for the inlet and outlet sections. Voltage usually decreases from inlet to outlet; current usually increases from inlet to outlet.

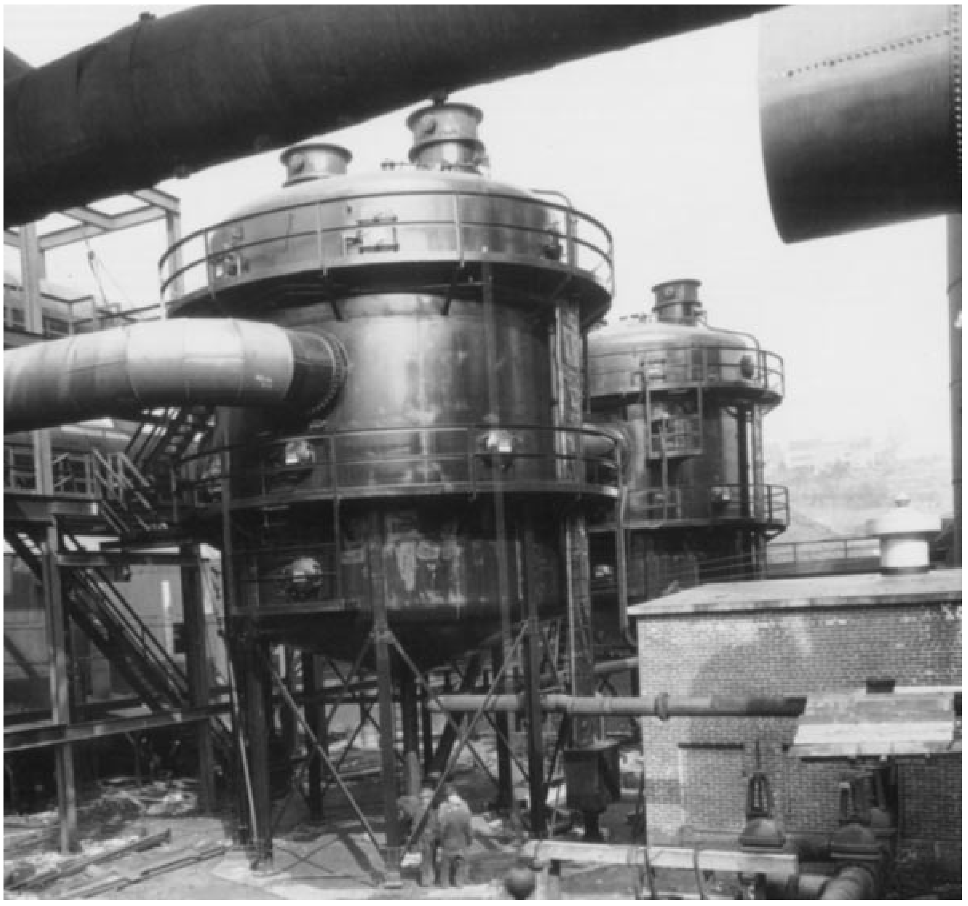

Figure 2. Two wire-tube precipitators. The gas enters at the bottom (not visible), flows up through individual small diameter tubes, and out the top sides. Electrical power to the corona wires is supplied from the two cylindrical metal enclosures on top of each unit. Collected liquid particles flow down through the tubes to drop into a hopper and drain below each unit. (Photograph courtesy Research-Cottrell, Inc., Somerville, NJ © 1997 by Research-Cottrell. All rights reserved.)

itators in the sense that most large precipitators are not as responsive to collector area as the Deutsch equation would imply.

All these equations are only approximations (5), and migration parameters are basically fitting parameters. They ignore many other processes that occur in precipitators (3, p. 96), but do show that plate area and gas volume are critical in determining the collection efficiency.

Mechanical Configuration

There are two principal geometries in industrial/utility precipitators: the tube type and the plate type. In the wire-tube precipitator, shown in Fig. 2, the wire corona electrode is coaxial with the tube, and the gas flow is along the same axis. In the wire-plate precipitator (Fig. 3), the electrodes hang vertically between parallel plates, and the gas flow is horizontal between the plates. In either case, the major components of the precipitator are the collection surfaces and the electrode system that includes the discharge electrode, an insulated support system, and a high voltage power supply. If the particles are collected dry, there must be a mechanical system to dislodge the particulate layer from the collection surfaces. This is often accomplished with a rapping system that periodically strikes the collections surfaces with a weight or hammer. The dislodged particles are collected in a hopper below the plates, from which they are evacuated for storage or disposal. Most tube precipitators are designed to collect liquid particles, but some plate precipitators ("wet" precipitators) are washed with internal sprays, rather than being rapped, for particle removal.

Discharge electrodes come in a wide variety. They can be classified as (1) weighted wire, with a weight attached to the bottom of the wire to keep it straight, (2) rigid frame, with the wires or other discharge elements suspended between frame members, (3) rigid mast, with a central member supporting discharge elements between cross-members, and (4) rigid discharge electrodes (single, rigid structures with discharge elements attached directly to the central member). Regardless of design, the electrodes all have elements with points or small radii of curvature to generate the high electric field needed for stable corona.

Electrostatic Precipitation Applications

The earliest application of electrostatic precipitation took place just after the beginning of the twentieth century. These early precipitators used high voltage transformers with synchronous mechanical rectifiers to produce the dc voltage needed for corona. Early uses for these precipitators included control of emissions from smelters and cement kilns (see AIR POLLUTION CONTROL). Since that period, the technology has steadily improved in performance and reliability, and precipitators are now used in a wide range of applications, including (2, pp. 8–24; 6, pp. 22–30; 7, pp. 2–6):

1. utility industry for the collection of flyash from coal and oil combustion

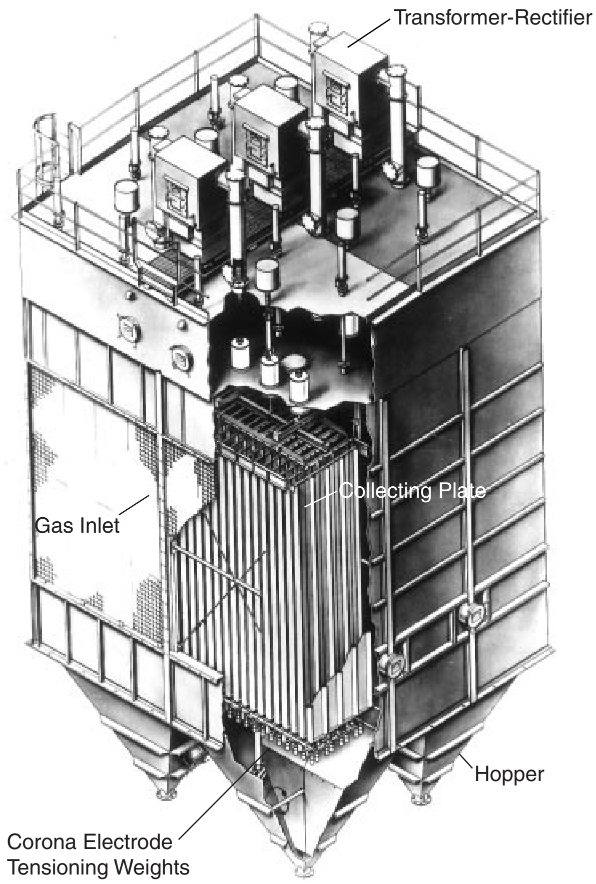

Figure 3. Wire-plate precipitator. The gas enters at the left face, passes through multiple lanes, and exits at the right face (not visible). The plates shown partially across the left face are perforated with many holes to provide uniform gas flow. Electrical power to three independent sections is supplied at the top. Plate rappers periodically dislodge the collected particles and allow them to fall into the hoppers below. (Illustration courtesy Research-Cottrell, Inc., Somerville, NJ © 1997 by Research-Cottrell. All rights reserved.)

2. iron and steel industries for particulate control
3. cement industry for particulate control in roasting ovens (see CEMENT AND BRICK INDUSTRY)
4. sulfuric acid manufacturing for the collection of sulfuric acid mists
5. pulp and paper industry for the collection and recycling of salt cake, crystals of sodium sulfate
6. nonferrous smelters, for both material recovery and particulate control
7. air cleaning for factories and offices
8. carbon black industry to aid in the production of carbon black

There are specialty applications, as well, but these eight constitute the majority of operating precipitators.

In the United States, the largest use of precipitators (size and number) is in the utility industry for control of particulate emissions. Most of the precipitators in Table 1 are examples from utility operations. In this demanding application, large volumes of flue gas, from 90 m^3/s to 950 m^3/s, are treated, and frequently high collection efficiencies, in excess of 99.5%, must be achieved. Yet, precipitators have long demonstrated the ability to meet such demands. The design of precipitators is discussed in some detail in later sections since high efficiency operation requires careful consideration of many conflicting goals.

Experience indicates that to achieve these efficiencies, gas velocities in the precipitator must be kept low, 1.5 m/s or lower, and the precipitator must be constructed with a high degree of sectionalization. Sectionalization means that only a small number of electrodes are energized by a single power supply and that only a small number of plates are rapped at any one time. In any precipitator that collects dry particulate material, some material is inevitably reentrained each time the collection surfaces are rapped. Sectionalization deals with this problem by placing multiple electrical and mechanical fields in the direction of flow, sometimes as many as ten fields. Most of the reentrained material from an early field is recaptured in following fields. Typically, the rate of collection in the last field is very low, and it is rapped infrequently, so that the amount of material lost to reentrainment is small compared to the amount entering the precipitator.

DETAILED EXAMINATION OF ELECTROSTATIC PRECIPITATOR OPERATION

The electrostatic precipitator is best described in terms of its major subsystems and their interactions. First of all, it is an electrical machine in which the generation of corona and provision of strong electric fields are essential for collecting particles. Second, it is a large mechanical device whose geometry has evolved over the years for providing the best collection of particles in the smallest volume. Third, for particle collection, particles must be charged and moved to the collection surfaces while large volumes of gas pass through the precipitator. These basic subsystems work together to provide the desired collection, but their operation can be upset by unusual conditions, poorly maintained mechanical equipment, or by changes in the properties of the particles being collected.

The understanding of precipitator operation has been aided immensely with the use of computer models. The number of variables and their interactions that must be considered create a complex situation. Operations that are easily described with a few equations have to be calculated repeatedly in order to accommodate changing conditions inside the precipitator, a job well suited for computers. Simple models of precipitator performance can be implemented with a few spreadsheet equations, but accurate models require the resources of modern personal computers.

Since precipitators consist of multiple parallel gas treatment paths, it is common to consider a single lane in the direction of flow as adequate for describing the precipitator operation. This single-lane approach describes almost all precipitator phenomena quite well, but even in one lane, the system is still complex.

Electrical Operation of the Electrostatic Precipitator

The production of corona as a source of ions is one of the two electrical functions of the precipitator; the other is creation of the electric field. The characteristics of high voltage coronas depend upon the electrical polarity, corona electrode geometry, properties of the gas, and properties of the electrode surface to some extent. In all cases, the corona is a Townsend electron avalanche sustained by secondary feedback (8).

An electron avalanche occurs when a free electron moves in a strong electric field. It gains enough energy between collisions with gas molecules to ionize the molecules with which it collides. This liberates additional electrons that participate in further ionizing collisions. The requisite conditions for the avalanche are (1) an electric field in excess of 3 MV/m (30 kV/cm) in air, (2) absence of gases that attach electrons strongly, and (3) an initial free electron. The avalanche mechanism can lead to a total electrical breakdown of the gas if it is not limited or stabilized. In precipitators, the stabilization comes from a combination of electrode dimensions and gas properties.

Corona Formation. The coaxial wire-tube precipitator, with a wire of radius r and a tube of inner diameter R is not only one of the simplest types of precipitators but also one of the easiest to analyze. If the outer tube is grounded and the inner wire is held at a voltage V in the absence of current, the electric field, E_0, at the surface of the wire is related to the voltage by (9, p. 32):

$$E_0 = \frac{V}{r \ln(R/r)} \tag{5}$$

The magnitude of the electric field, $E(z)$, for any value of z between r and R is given by

$$E(z) = \frac{E_0 r}{z} \tag{6}$$

The applied voltage can be made sufficiently high so that the electric field at the surface of the wire and for some distance into the gap is larger than 3 MV/m. Under such conditions, a free electron (from a passing cosmic ray) would create an avalanche.

If the wire is positive, the electrons move toward the wire and are neutralized on the wire surface. If the wire is negative, the electrons move away from the wire into regions where the electric field is too weak to support the avalanche. Each avalanche would produce only a single burst of electrons and ions, if there were no mechanisms to liberate more free electrons in the high field region.

One mechanism for sustaining the corona is photoionization. When an electron and a positive ion recombine, the atom emits ultraviolet radiation to remove the energy of recombination. This radiation can ionize a similar molecule some distance away. Since there are a multitude of photons in the initial avalanche, some electrons are likely to be liberated at the proper distance to begin a new avalanche.

When photoionization sustains the multiple avalanches of the corona, a "glow" corona is formed. For positive polarity, the glow forms a tight sheath around the wire about 1 mm thick, while for negative polarity, the glow appears as rapidly moving discharges along the length of the wire, forming a sheath about 10 mm thick.

The lowest voltage at which corona occurs can be used with Eq. (5) to calculate the field at the surface of the wire, the "critical" field for corona onset. The critical field for glow corona is a function of wire radius (but not material) and gas density, as given by

$$\begin{aligned} E_c &= 3.126 \times 10^6 \left(\delta + 0.0301\sqrt{\frac{\delta}{r}}\right) \\ \delta &= \frac{298}{T} P \end{aligned} \tag{7}$$

where E_c is in V/m, r is in meters, T is in kelvin, and P is in atmospheres. This equation is valid for negative corona; for positive corona, the value 0.0301 would be replaced by 0.0266. The form of this equation is due to Peek (10).

For negative polarity, positive ion impact can also liberate free electrons from the wire surface (see IMPACT IONIZATION). Each electron avalanche away from the wire leaves behind a cloud of positive ions that are attracted to the wire. Some positive ions impact the surface with enough energy to liberate more free electrons. Once a small area on the wire becomes effective for impact ionization, successive avalanches will tend to originate at the same spot, creating a "tuft" corona (11). This ion impact mechanism is so efficient that the critical field for tuft formation is typically 60 percent of the value given in Eq. (7); under most conditions, glow corona will eventually collapse into tuft corona.

For positive corona, positive ions left over from the electron avalanches move away from the wire to fill the interelectrode gap. For negative corona (either glow or tuft), the electrons from the avalanche are captured by electronegative molecules (typically oxygen) to form negative ions that continue to move away from the wire. In industrial flue gases, more acidic molecules (sulfur dioxide, sulfuric acid) will rapidly collect electrons or strip them from oxygen ions to form the primary current carrying ions in the gas.

The corona itself extends into the gap only as far as the electric field is able to support the avalanche. However, corona serves as an almost unlimited source for ions that continue across the gap. Without additional stabilization, the current from a wire would increase without limit. The stabilization is provided by the accumulation of charged ions between the wire and the collection electrode, called the ionic space charge.

The ionic space charge produces an electric field that opposes that applied field. This opposing field stabilizes the corona and permits the voltage to be increased well above the corona onset. With each increase of voltage, the corona injects more ions into the electrode gap, but the increased space charge prevents the number of ions from rising indefinitely. The difference between a corona device and other gas discharge devices, such as neon lamps or thyratrons, is that the electrode spacings and gas pressures are very different; ionic space charge can stabilize the corona, but not the discharge in smaller devices.

Current Density and Voltage. The voltage–current density relationship is important because it establishes the possible range of operation. (Current density is used for describing precipitator operation because it is independent of the number of corona electrodes and plate area.) For voltages below the corona onset value, there is no current, no particle charging, and no collection of particles. Once the voltage increases to the point of repeated sparking, there can be no further increase. The precipitator must operate between these limits with sufficient current density to provide particle charging and collection.

The corona onset voltage, V_c, in the wire-cylinder is calculated by direct integration of the electric field to obtain

$$V_c = E_c r \ln\left(\frac{R}{r}\right) \tag{8}$$

For a single wire between plates, a similar relation holds:

$$V_c = E_c r \ln\left[\frac{1+\cos\left(\frac{\pi r}{2b}\right)}{1-\cos\left(\frac{\pi r}{2b}\right)}\right]^{1/2} \tag{9}$$

where b is the wire-plate separation. When multiple wires are between plates, there is a mutual coupling effect that raises the corona onset voltage for all the wires. When the wire-wire separation is greater than twice the wire-plate separation (a common configuration), the coupling effect is only a few percent of the single wire corona onset voltage.

Above the corona onset voltage, the relationship between current density and voltage is

$$\begin{aligned} V &= V_c + E_c r\left[a - 1 - \ln\left(\frac{a+1}{2}\right)\right] \\ a &= \sqrt{1 + \frac{j_0 x}{\mu\epsilon}\left(\frac{x}{E_c r}\right)^2} \end{aligned} \tag{10}$$

where j_0 is the current density at the collector, μ is the ion mobility, ϵ is the permittivity of space, and x is the wire-collector separation distance (R for the wire-cylinder or b for the wire-plate). This relationship is exact for the wire-cylinder (9, p. 34), where the current density is equal over the whole collector surface, and nearly so for the wire-plate for the central current density, the current density directly under the corona wire on the plate.

A fairly accurate estimate of the current density for a given voltage can be obtained with the equation:

$$j_0 = \frac{\mu\epsilon}{x^3}(V^2 - V_c^2) \tag{11}$$

This approximate relation matches Eq. (10) best at the higher values of j_0. For critical work, Eq. (10) is preferred.

In the wire-plate geometry, the current density along the plate varies approximately as

$$j(\theta) = j_0 \cos^n(\theta) \tag{12}$$

where the angle θ is measured from the perpendicular line from wire to plate, shown in Fig. 4, and the value of n is 4–5 (12). Eq. (11) and Eq. (12) are inferred from the insights of Sigmond (13) and represent nearly universal corona behavior. That is, the ions are so dense at the wire that mutual repulsion dominates all other effects (see SPACE CHARGE AND SPACE CHARGE MEASUREMENTS), leading to a voltage dependence that follows Sigmond's saturation law (with a correction for the corona onset voltage) and an angular dependence that approaches a straight line expansion away from the corona wire.

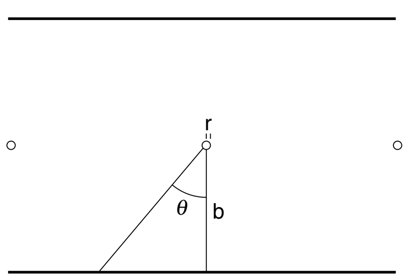

Figure 4. Wire-plate geometry with wire radius r and wire-plate spacing b. The electric field and current density at the central location ($\theta = 0$) are almost the same as for the wire-tube precipitator.

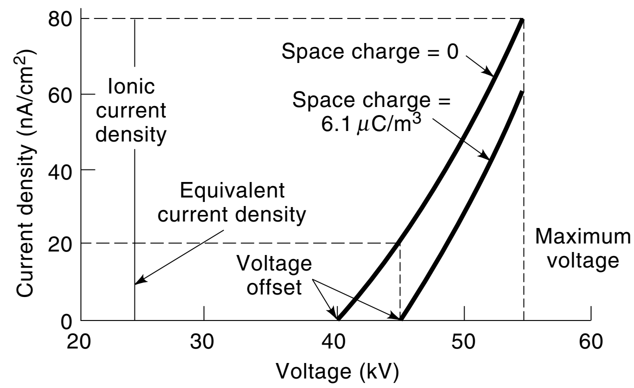

Figure 5. Shifting of the V–j curve with particulate space charge. The 5 kV offset is equivalent to a current density of 20 nA/cm², which reduces the amount of real ionic current that can flow at a given voltage.

Charged particles in the precipitator complicate the voltage–current density relation to the point that there is no exact representation of the V–j curve. A uniformly distributed cloud of particles moving through a wire-plate precipitator will produce an electric field that opposes the formation of corona, raising the corona onset voltage by an amount:

$$\Delta V = \frac{S}{\epsilon}\frac{b^2}{2} \tag{13}$$

where S is the total particulate space charge (C/m³). In addition, the space charge enhances the electric field toward the collection plate and so assists in the movement of ions. This results in a steepening of the V–j curve. A reasonable estimate of the effects of space charge is obtained by assuming that it is an equivalent current density added to the ionic current density, as illustrated in Fig. 5. As the space charge increases, the real ionic current available at a given voltage decreases. In extreme cases, the ionic current may be suppressed or "quenched" altogether.

The electric field around the wire establishes the charging conditions and provides the motive force for collecting particles. The presence of ions and particulate space charge modify the Laplacian (zero current) field given by Eq. (6).

Electric Field. The electric field with ionic current and without space charge in the wire-cylinder is given by

$$E(z) = \left[\left(\frac{E_0 r}{z}\right)^2 + \frac{jz}{\mu\epsilon}\left(1 - \frac{r^2}{z^2}\right)\right]^{1/2} \tag{14}$$

Here, j is the current density crossing an imaginary cylinder at radius z. The Laplacian portion of the field ($j = 0$) decreases with distance from the central wire, but the ionic space charge increases the field as the outer cylinder is approached. At the outer cylinder, with $z = R$ and neglecting the correction term for the wire radius, the field becomes

$$E(R) = \left[\left(\frac{E_0 r}{R}\right)^2 + \frac{j_0 R}{\mu\epsilon}\right]^{1/2} \tag{15}$$

A similar expression works for the wire-plate geometry at the central location:

$$E(b) = \left[\left(\frac{E_0 \pi r}{b}\right)^2 + \frac{j_0 b}{\mu\epsilon}\right]^{1/2} \tag{16}$$

These expressions are for single electrodes. In the wire-plate geometry, adjacent electrodes make a contribution to the Laplacian term, increasing it by up to several percent for closely spaced wires. In the wire-plate geometry, the electric field along the plate varies approximately as

$$E(\theta) = E(0)\cos^n(\theta) \tag{17}$$

where the value of n is 2.

Particulate space charge adds a constant amount to the field at the plate of Sb/ϵ, and there is no angular dependence for this component of the field. As a result, the electric field becomes

$$E(\theta) = E(0)\cos^n(\theta) + \frac{Sb}{\epsilon} \tag{18}$$

Strictly speaking, the space charge will increase from charging as the particles approach the electrode and decrease as some of the particles are collected near the electrodes. These effects are real, but small, for the amount of time particles spend near any one electrode.

The interest in the values of field near the plate comes from the assumption that the near-plate region is where the collection of particles takes place. The electric field in the interelectrode gap is important in determining the charging conditions, but some average value, computed from Eq. (14), is almost always used.

Voltage Wave Forms. Although the precipitator uses high voltage dc to operate, the wave forms may vary considerably. Older precipitators were often energized with unfiltered half-wave rectified dc, probably for economic reasons, since a single transformer-rectifier (TR) could energize two separate sections. Newer precipitators use full-wave rectified dc for all sections. Although power supply filtering is rarely used, the precipitator itself is a large capacitor and smooths the wave form somewhat. Some TR controllers now interrupt the primary ac voltage for several half-cycles to provide an intermittent energization, with the goal of reducing the current consumed while keeping the peak voltage high.

Generally, the average current density for a given average voltage is not sensitive to the wave form. The current density-voltage characteristic, Eq. (11) for example, is linear enough over the normal operating range that the differences in wave form do not produce different curves. Wave form does dramatically affect the peak voltage and peak current density.

Equation (10) and Eq. (11) are approximately valid whether or not the voltage is changing with time (at power line frequency) because the ions can cross the electrode gap in about a millisecond. Therefore, when the voltage on the electrodes rises to its peak value, the current density also rises to a peak value that may be several times its average value, depending on the wave form. The electric field also follows the voltage and current density changes. The phase relationship between voltage and current may be modified by the capacitance of the system in addition to the ion transit time.

Some precipitator phenomena do not respond rapidly enough to be affected by the peak values, but the phenomenon of sparking is directly attributed to the high electric fields that exist at the peak of the voltage wave form.

Sparking. Sparking is a complete breakdown of the electrode gap with enough gas ionization to effectively short circuit the precipitator power supply. Sparking is usually initiated by the formation of positive streamer corona at one electrode that extends to the other electrode. The streamers propagate by photoionization into the gap; their repeated passage over the same volume heats the gas, increases its conductivity, and leads to the catastrophic spark. The streamers will form and propagate when the electric field is in excess of 0.5 MV/m (5 kV/cm). The temperature-reduced pressure dependence of the formation field is moderate, varying roughly as $(pressure)^{3/2}$ (14). This means that altitude, as well as the temperature, of the precipitator will affect the field for sparking noticeably. The moisture dependence is also fairly strong, such that the amount of water in a combustion gas stream might raise the field for sparking by 1 to 2 kV/cm.

All control systems for TR sets are designed to turn off the voltage for a few cycles after a spark occurs to protect the supply and the precipitator electrodes from damage. This does shut down the whole electrical section served by the set for a few tenths of a second and represents a period of time when little collection (except for the space charge field) takes place. Repeated sparking at the same spot on a wire is one of the primary causes of electrode failure.

Gas Composition Effects. It has been recognized that the moisture content of the gas affects the sparkover voltage significantly. Other elements in the gas composition can affect the electrical operation equally strongly. Ion mobility, defined as the ratio of ion velocity to electric field, is characteristic of each type of ion. Small, compact ions have high mobilities, while large, complex ions have smaller mobilities.

In air, the negative ions that carry current are typically hydrated oxygen molecules, with a reduced mobility of about 2×10^{-4} $m^2/V \cdot s$. In precipitators controlling emissions from coal-fired boilers, sulfur oxides form the dominant ions because their acidity allows them to capture electrons from the oxygen ions. Sulfur dioxide (SO_2) has a mobility of about 1.80×10^{-4} $m^2/V \cdot s$. at very low concentrations in air (15), but about 0.41×10^{-4} $m^2/V \cdot s$ at high concentrations (9, p. 24). The crossover from low- to high-concentration behavior occurs at about 400 μL/L (16). Ion mobility is also a function of gas density (a combined pressure and temperature effect). Consequently, it is possible for seemingly minor changes in gas composition and conditions to affect the operation of the precipitator by a large amount.

Mechanical Design of the Precipitator

The mechanical design and construction of precipitators affects their performance in subtle ways. In the wire-cylinder precipitator (see Fig. 2), the collected particles must be removed by flowing downward against the upward gas flow. This limits the use of tube precipitators to collecting liquid particles or providing for offline cleaning. In the plate-type precipitator (Fig. 3), there are three axes of movement for particles: along the horizontal gas flow, transverse to the flow towards the plates, and vertically downward towards the hoppers. This allows the collected particles to be removed without serious reentrainment in the gas flow. Most of the following discussion concerns plate-type precipitators.

Overall Dimensions. The sizing of a precipitator for high efficiency particle collection for coal flyash aims toward a treatment time of 4 to 10 s with a gas velocity in the direction of flow of no more than 1.5 to 1.6 m/s. Higher velocities tend to cause increased rapping losses and continuous erosion of the collected particles. Other types of particles will modify these criteria.

The overall length is then optimally in the range 6 to 16 m. Invariably, other constraints limit the length: fitting into an existing space, costs of land, arrangements of ductwork, and so on. The lane height and overall width need to be adjusted to accommodate the volume of gas and the treatment time.

The lane height is also constrained by considerations of electrode alignment and the total distance the collected particles must fall to reach the hoppers. Common lane heights range from 9 to 12 m. In retrofit situations, it is often easiest to add height to the plates because the footprint of the precipitator does not need to be modified. In those situations, even taller plates might be used, but the rapping losses might become unacceptable.

The total width has no effect on the operation of the precipitator, except for the details of mechanical construction. The ratio of width to height in large precipitators varies from 1 : 1 to 8 : 1. Wider precipitators are usually subdivided into separate chambers for better mechanical integrity.

Within the optimal treatment times, there is some latitude for choosing the plate spacing (lane width) and collector area. Wider plate spacings (30 cm to 40 cm) provide more tolerance for electrode alignment problems and require less plate material but always require higher voltages and may encounter problems with particulate space charge. Narrower plate spacings (22 cm to 27 cm) are more traditional, provide more plate area for collection, and operate at lower voltages but are more critical to align and maintain.

Electrode Design. Long electrodes are difficult to keep aligned between the plates. Wire electrodes are often weighted to keep them vertical and taut; the weights may be guided at the bottom to suppress swaying. With frame electrodes, wires are stretched across a rigid tubular frame to provide alignment; the frame itself must be carefully constructed to remain aligned. Rigid electrodes and mast electrodes provide a strong tubular spine along which corona electrodes are placed at close-spaced intervals; these electrodes are often supported on alignment frames at both top and bottom.

All the electrode designs require that the electrodes be isolated from ground by strong insulators. The insulators must not only support the gravitational load of the electrodes but also dynamic loads if the electrodes are rapped to remove deposited particles.

Plate Design. Tall plates suffer some of the problems that the electrodes do. Even when suspended from the top, warpage may occur because of manufacturing flaws, thermal gradients, overheating, or other causes. Many plates are designed with stiffening ridges, at right angles to the plate surface, in them. The ridges extend into the gas stream somewhat and affect the gas flow. Sometimes, the stiffeners are also intended to shield the deposited particles from the gas flow to reduce erosion of the deposits.

Sectionalization. As the need for more efficient collection grew, it became apparent that parts of the precipitator needed to operate in different regimes. Near the inlet, the particle concentrations are high and produce a high space charge. This requires a high voltage to drive the corona current. Near the outlet, most of the particles have been collected, and a high voltage will produce very large corona currents and sparks. By breaking the precipitator into shorter, independent sections, each section can operate at its own optimal conditions. Sectionalization also provides redundancy to protect against equipment failures. A four-section precipitator may lose one section to a failure and still operate fairly well; a single-section precipitator fails totally.

Each section is much shorter in the direction of flow than it is tall. This makes collected particles fall a long distance toward the hoppers, during which reentrainment may occur. Plates in a section may extend the full length of the section in the direction of flow or may be smaller subunits closely fitted together. Sometimes, the individual subsections are rapped independently.

Access Lanes. There are usually access walkways running the width of the precipitator between sections to allow for maintenance and inspection. Particles emerging from one section are thoroughly mixed in the access lanes before passing into the next section. The dimensions of the access lanes allow large turbulent eddies and cross-flows from one part of the precipitator to another to form. Even if care is taken to assure low turbulence within the lanes, the access lanes change the flow structure and homogenize the particle concentration.

Sneakage. The requirement for electrical isolation of the high voltage electrodes means that rather large spaces must be allowed at the top and bottom of the lanes to prevent sparking. These spaces provide the opportunity for particle-laden gas to bypass the collection zones, a phenomenon called sneakage. Internal baffles are often used to suppress the sneakage flow or redirect it toward the active collection zone, but the clearances must still be maintained.

To some extent, the sneakage flows are driven by the pressure drop along the length of the precipitator. The presence of plate stiffeners produces a back pressure that is partially relieved by gas flows out of the top and bottom of the lane. A simple model of the pressure drop (17) shows that increased stiffener protrusion into the lane increases the sneakage flow and that taller plates show proportionally less sneakage than shorter plates. Sneakage flows represent losses of efficiency and may also allow particles to contaminate areas that should be kept clean.

Particle Collection

Particle collection is the primary goal of precipitation, but in many aspects, it can be discussed independently of the electrical and mechanical aspects of the precipitator. For much of the time in the precipitator, the particle cloud is so dilute that the charging and collection do not affect the electrical operation of the precipitator. Once the operation of the precipitator is understood for dilute concentrations, then the concentrated regime can be addressed.

Particle Size Distributions. The particles that the precipitator must collect are rarely all of the same size. The processes that produce particles (combustion, chemical reactions, mechanical processes) make them over a range of sizes, called a size distribution (18). The size distribution describes the numbers of particles of a specific size that would be found in a representative sample. For precipitation, size distributions are considered in terms of number or mass. Mass distributions are easily measured by aerosol collection equipment, such as cyclones or impactors, while numerical computations are most easily carried out in terms of number distributions. If the particles are spherical, the conversion between mass and number distributions are straightforward.

Figure 6 shows a particle number and mass size distribution of the type often found in coal-fired precipitator applications. The mass distribution has a maximum value at about 10 μm diameter, and the shape is roughly lognormal (normal in the logarithm of the independent variable). Approximately half the particulate mass is in particles larger than 10 μm, which are easily collected; the remaining mass below 10 μm is harder for the precipitator to collect. At the upper end of the mass distribution, the large particles are fewer than might be expected because they have settled in the furnace and ducts. At the lower end of the distribution, a condensation aerosol may form from material volatilized in the furnace (silica or sulfuric acid, for example). The number distribution is heavily weighted toward small particle diameters because the mass of a particle varies as the cube of its diameter.

A number distribution strongly peaked at small particle sizes (called a submicron mode) can present problems for the precipitator because each particle must be charged in order to be collected. The ions used for charging the numerous small particles are not available to charge the larger ones, and the strong particulate space charge limits the ionic current. Fortunately, when it is known that a submicron mode is likely to be present, the electrode design can be altered to compensate for the problem.

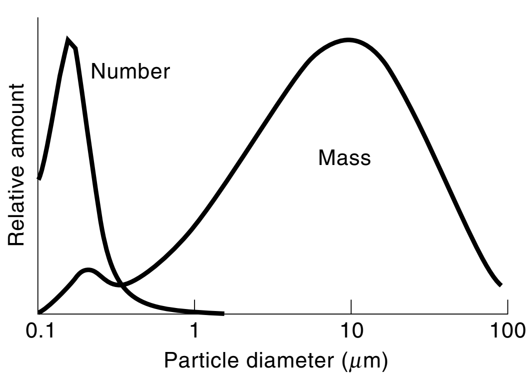

Figure 6. Number and mass particle size distributions typical of coal-fired precipitator applications. The small mass peak at 0.2 μm is a condensation aerosol and may not be present in all situations.

Particle Charging. Particle charging in precipitators has been a topic of interest for decades because ionic charging covers nearly the full range of parameters that can be modeled. For large particles, the field charging (convection) model gives an appropriate description. For small particles, diffusion models give an appropriate description. In between, composite or numerical models must be used to adequately describe the charging. An excellent summary of the classic field charging model is in (9, pp 58–63), and a comparison of all the classic precipitator charging models in nondimensional form is made in (19). When an ion is near the surface of a particle, it is attracted to the particle by image forces, and the concentration of ions at the surface is zero. Field and diffusion charging models describe the transport of ions to the vicinity of the particle surface.

In fact, the field charging model is only an approximation of the true charging relationship; diffusion effects can be observed well into the classical field charging regime. Convection along the electric field (field charging) delivers ions to the neighborhood of the particle, but diffusion across the concentration gradient at the surface determines the charging current (20).

Particle Charging Theory. The particle charging equations are simplified if expressed in nondirectional form (19). The nondimensionalized terms are the particle potential, electric field, and charging time. (Other quantities are also needed for the development of the theory (21), but these three are sufficient to understand the results.) The terms are defined as follows:

Self potential of the particle, ν (also called the particle charge):

$$\nu = \frac{ne}{4\pi\epsilon a} \Bigg/ \frac{kT}{e} \tag{19}$$

where n is the number of elementary charge units e, ϵ is the permittivity of air, a is the particle radius, k is Boltzmann's constant, and T is the absolute temperature. This expression is the ratio of the electrostatic potential to the quantity kT/e, the thermal potential. The thermal kinetic energy of the ions in the gas divided by e is about 26 mV at room temperature. Because ions have this average thermal energy, they can overcome repulsive forces near the particle and reach the particle's surface, even when the classical convective field equations forbid such occurrences.

Electric field, w:

$$w = aE \Bigg/ \frac{kT}{e} \tag{20}$$

where E is the uniform applied electric field. The product aE is the potential across the radius of the particle. When this product is smaller than thermal potential, diffusive effects will dominate the particle charging.

Time, τ:

$$\tau = \frac{\rho \mu t}{\epsilon} \tag{21}$$

where ρ is the ion density, μ is the ion mobility, and t is the actual charging time. The quantity ρt is often termed the ion exposure time.

With these definitions in hand, the charging rate for classical field charging is

$$\begin{aligned} \frac{d\nu}{d\tau} = F(\nu, w) &\equiv \frac{3w}{4}\left(1 - \frac{\nu}{3w}\right)^2, \qquad \nu \le 3w \\ &\equiv 0, \qquad \nu > 3w \end{aligned} \tag{22}$$

where $3w$ is commonly called the unipolar saturation charge; it is the upper limit of charge that can be attained by the field charging mechanism. The field charging rate is named $F(\nu, w)$ for convenience in referring to it. The value 3 comes from the assumption of conductive particles. (For most precipitators, this assumption is reasonable.)

The field charging model has a strong initial charging rate, $3w/4$, that becomes zero at $\nu = 3w$. The larger the particle (radius a), or the stronger the field, (E), the greater the charging rate is. When $\nu = 3w$, the charge on the particle is

$$ne = 12\pi\epsilon a^2 E \tag{23}$$

Large particles, therefore, acquire very large charges in the precipitator and can be easily collected.

The classical diffusion charging rate in nondimensional notation is

$$\frac{d\nu}{d\tau} = \mathrm{Be}(\nu) \equiv \frac{\nu}{\exp(\nu) - 1} \tag{24}$$

This function is called the Bernoulli function, designated here Be(ν), because it is a generating function for Bernoulli numbers. The initial diffusion charging rate is 1 and becomes exponentially smaller as the charge on the particle increases, without ever completely ceasing.

The relative importance of the field and diffusion contributions to charging can be estimated by comparing the initial charging rates. Once the saturation charge is reached, however, field charging ceases, but the diffusive component remains. The method of combining the two charging rates determines the accuracy of the overall particle charging model.

As long as the particle charge ν is less than $3w$, some of the particle's surface is at the same potential as the surrounding space. This means that a portion of the surface receives a diffusive current in addition to the field charging. In addition, that diffusive current is the same as for a particle of zero charge in the absence of the field. Taking the fractional area receiving the diffusive contribution into consideration, the charging rate becomes

$$\begin{aligned} \frac{d\nu}{d\tau} &= F(\nu, w) + f(w)\mathrm{Be}(0), \qquad \nu \le 3w \\ &= f(w)\mathrm{Be}(\nu - 3w), \qquad \nu > 3w \end{aligned} \tag{25}$$

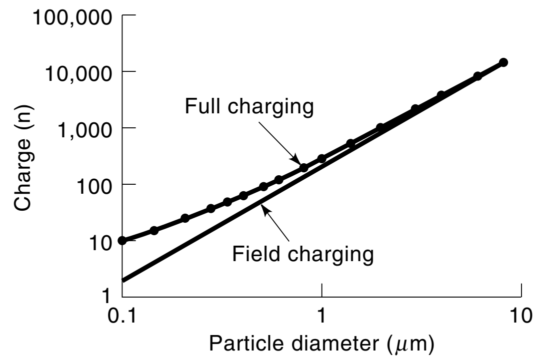

Figure 7. Computed particle charge (number of electrons) on particles in a precipitator under normal operating conditions ($E = 5 \times 10^5$ V/m, $j = 1.2 \times 10^{-5}$ A/m^2, time = 1.9 s). With the high electric field, sparking occurs in the precipitator but does not affect the charge. The straight line computed by field charging alone shows the dependence on the square of the particle diameter and an increasing discrepancy from real charges below 3 μm.

where the area fraction, $f(w)$, is described by the equation:

$$\begin{aligned} f(w) &= \frac{1}{(w + 0.475)^{0.575}}, \qquad w \ge 0.525 \\ &= 1, \qquad w < 0.525 \end{aligned} \tag{26}$$

When the particle charge reaches $3w$, the field charging rate becomes zero, but the diffusive contribution continues to raise the particle potential above $3w$, at a decreasing rate.

Figure 7 shows some particle charges computed in modeling a precipitator. Even though the electric field changes in time (because of sparking) and in space (as the particles pass each corona wire), the charge on each particle increases continuously because there is no way for charge (ions) to leave a particle once they have been captured.

Charging at High Particle Concentrations. Once the charging problem for dilute particles is understood, it is possible to extend the modeling to more concentrated particle clouds. Particulate space charge is the sum of all the charges on all the particles within a volume of space. Eq. (13) shows that the space charge shifts the corona onset voltage upward and reduces the current density. Each shift reduces the ions available for charging and decreases the charging rate. Particles receive only a fraction of the charge that they would under more dilute conditions. Nonetheless, some particle charging does occur, even under these reduced-current density conditions. The charging is slower than under dilute conditions, and it is more difficult to calculate. The charging model is still correct, but the local ion density and electric field change rapidly with each position inside the precipitator.

Particle Motion. Charged particles experience a force in an electric field of neE. In still air, a particle accelerates until viscous drag in the air exactly opposes the electric force, at which time the particle moves with a constant drift velocity, given by

$$v(a) = \frac{neEC}{6\pi\eta a} \tag{27}$$

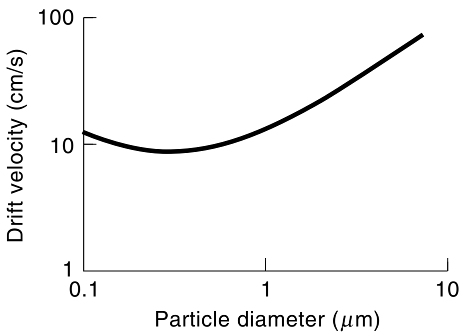

Figure 8. Computed particle drift velocities in a field of 5×10^5 V/m. The minimum in velocity typically occurs in the range 0.3 μm to 0.5 μm. Although particle velocities greater than 100 cm/s are calculated for larger particles, other factors related to the particle's Reynolds number need to be taken into account to compute the velocity accurately. Even so, such particles are collected very efficiently.

where C is the Cunningham slip correction factor, and η is the viscosity of the gas. This is an expression of Stokes' law (18), relating the particle velocity to its viscous drag. Since the particle charge increases roughly as a^2, and the drag increases as a^1, the particle velocity increases with the radius a. The slip correction factor, C, accounts for the fact that as particle diameters become comparable to the mean free path of the gas molecules, the particles slip through the gas with less hindrance (22). As a result, the particle velocity increases for particles smaller than about 0.5 μm diameter. In turbulent gas flows, this equation indicates the particle velocity with respect to the local gas velocity.

Particle drift velocities corresponding to the charging conditions in Fig. 7 are shown in Fig. 8. Most of these velocities are well above the characteristic precipitator velocities in Table 1, suggesting very effective collection. Near the minimum drift velocity, the collection efficiency is the poorest.

Gas Flow in Precipitators. As indicated before, the target velocity for the gas flow in precipitators is 1.5 m/s or slower. For the lane widths commonly encountered, 0.2 to 0.4 m, computed Reynolds numbers range from 4500 to 15000, well above the threshold for turbulent flow (2000 to 2200), but not indicative of extremely turbulent conditions. If the gas flow entering a lane is nonturbulent, turbulence may not fully develop until most of the lane has been traversed. Plate stiffeners, referred to in the section on mechanical design, do induce turbulence in the flow, and once established, the turbulence remains constant.

Although much research has been devoted to the study of low-turbulence precipitators, it has been found that corona and particulate space charge induce motions in the flow stream equivalent to turbulence. Ions and charged particles drag gas toward the collecting plate, an effect called corona wind. Near the plate, the gas must change direction and move away from the plate, even though the ions and particles continue towards the plate. This motion creates a large-scale eddy that carries some of the particles back toward the center of the lane.

Local Particle Collection. Turbulence tends to homogenize the particle concentration across each lane, while the strong electric fields near the wires and directly under them move the particles toward the collecting plates. When the turbulent eddy velocities are lower than the particle drift velocity, the particle can travel to the plate and be captured.

The collection of particles can be modeled as a series of collection zones under the corona wires, followed by mixing zones between the corona wires. The classical Deutsch relation for a given particle size can be written as

$$p(a) = \exp(-v(a)/\omega_p) \tag{28}$$

where p is the penetration for particle size a, v is the drift velocity, and ω_p is the specific precipitator velocity. Penetration is $1 - eff/100$, the fraction remaining after collection; emissions from the precipitator are proportional to the penetration. However, a better collection model has been found to be

$$p(a) = \left[1 - \frac{v(a)}{N\omega_p}\right]^N \tag{29}$$

where N is the number of collection zones or wires in the precipitator (23). Equation (29) is a two-term series approximation to Eq. (28), but it actually predicts precipitator collection better than the Deutsch equation does, a finding related to the relatively low turbulence in precipitators. The Deutsch equation does not allow all the particles to be collected in a precipitator, but Eq. (29) does. If the drift velocity exceeds $N\omega_p$ the penetration for that particle size is zero.

The total collection performance for a section must be evaluated by summing over all the particle sizes in the particle size distribution. The penetration of each particle size determines how many particles of that size appear at the outlet of the section, and the aggregate total allows the effective migration velocity, ω, to be calculated, if desired. The particle size distribution will change from section to section as the more easily collected large particles are removed from the gas.

Rapping. The collected (solid) particles build up a dust cake on the plates that must be removed periodically. It is usually desirable to keep the layer thickness between 2 and 5 mm to obtain good cake cohesion when the material falls into the hopper. In the inlet section, the layer thickness may increase 6 to 8 mm/h, necessitating frequent rapping. In the later sections, longer rapping periods are generally used.

Rapping is intended to break the dust cake loose from the plate and allow it to fall as a unit until it reaches the hopper or is trapped under another corona wire. Even if these conditions hold, some rapped dust will fall off the trailing edge of the section and have to be captured downstream. The desirable dust cake thickness should decrease with each section downstream of the inlet to reduce these rapping emissions, but the rapping period should still be long enough to allow a cohesive dust cake to form.

Deficiencies in Precipitator Operation

There are aspects of precipitator operation that interfere with the collection and disposal of particles. Some of these occur with every precipitator, while others are specific to certain types of particles. Improper maintenance of the precipitator will also produce problems of operation.

Rapping Losses. The rapping process allows some collected material to be lost into the gas stream on its way to the hoppers. Even though the reentrained material may be caught in the later sections, when they are rapped, some of that material will be reentrained. In the last section of the precipitator, the reentrained material leaves the precipitator and becomes part of the total emissions. From measurements of precipitator emissions with rappers on and off, it has been estimated that the rapping contributes 15 to 65% of the total mass emissions, depending on the precipitator's configuration.

A model (23) of the rapping process gives the fraction reentrained from each plate as

$$RR = \frac{H}{L}\frac{(0.18v_g)^2}{g\Delta x} \tag{30}$$

where H is the plate height, L is the plate length in the direction of flow, v_g is the average gas velocity, g is the acceleration of gravity, and Δx is the distance in the direction of flow between wires. The factor 0.18, obtained from fitting the model to several measured cases, predicts gas velocity near the plate as a function of the average velocity. The model gives rapping reentrainment factors approximating real precipitator operation. It shows that rapping losses increase dramatically with gas velocity and points out the importance of good gas flow conditions.

Velocity Maldistribution. Even though the average gas velocity through the precipitator may give the proper treatment time, if there are regions of high and low gas velocity, the precipitator will not work as well as it should. In the low velocity regions, the precipitator will actually exceed the average collection performance, but in the high velocity regions, the performance will be so degraded that the overall performance will suffer.

Part of the degradation in the high velocity regions is due to reduced charging and collection time for the particles, but a larger part of the degradation comes from the increased rapping reentrainment where the gas velocity is higher. There are some subtle effects in the low velocity portions as well. Sparking may occur because the particle space charge is so effectively removed. The dust cake will accumulate faster because of the better collection and may not be rapped at the appropriate intervals, leading to downstream overload conditions when the plates are rapped.

Modern precipitator design calls for the gas velocity at the face of the precipitator to be made uniform to within 15 percent rms. Precipitators that operate outside that range may have their performance improved with correct flow distribution. In cases with loosely cohesive dust, the flow conditions for good performance may be even more stringent.

Continuous Erosion of Dust Cake. In some cases, it has been found that the dust cake experiences continuous erosion between rapping intervals. This is a function of the cake cohesivity and gas velocity near the collecting plates. Low resistivity also contributes to the erosion problem because if the electric field (product of current density and resistivity) in the dust layer is lower than the electric field in the gas, there is a surface charge that exerts a force pulling the cake toward the interelectrode gap. Only the dust layer cohesion opposes this force. (This low resistivity effect forms the basis for using a precipitator as an agglomerator in carbon black processing.)

At higher resistivities, when corona current flows through the dust cake, strong forces develop to compress the cake, and erosion is unlikely. In adjacent areas without current flow, particles may be collected by the electric forces, but the cake is much looser and more easily eroded. The patterns of corona current clamping are determined by the electrode design (24). When continuous erosion is a problem, reductions of velocity, changes in electrodes, and the use of additives to improve cohesion are potential solutions.

Back Corona. If the electric field in the dust layer from the flow of corona current becomes large enough, the field can support corona generation in the interstices of the dust layer. The corona in the layer injects ions of opposite normal polarity back into the interelectrode gap, hence the name back corona. The precipitator is intended to be unipolar (charge of one sign only). When ions of both polarities are present, they charge particles in opposition, so that the net charge is much reduced below the full unipolar charge.

It has been found that the critical field for back corona formation in coal flyash is about 5×10^5 V/m. This is much smaller than the 3×10^6 V/m required for corona at the high voltage electrode. Two factors assist the formation of back corona at lower fields in the dust. First, current flow between touching particles is focused into very small areas at the point of contact. This focusing creates high electric fields that make microsparks in the particle-particle gaps. Second, the close confines of the pores in the dust cake assure that photoionization and ion impact events will be very effective at producing secondary electrons to sustain the ionization process.

Back corona has two deleterious effects on precipitator operation. First, the injection of opposite ions increases the current and lowers the operating voltage; the electric field is reduced as well. As a result, both particle charging and collection suffer in direct proportion to the field reduction. Second, the presence of the positive ions reduces the net charge on all particles. The negatively charged particles vigorously attract the positive ions, partially neutralizing them. Particle charging models can all account for bipolar ionic charging; all predict zero net charge if the bipolar ionic currents are equal.

Since back corona generation cannot proceed without the normal corona, the back ionic current will always be a fraction of the forward ionic current, and most particles will, therefore, carry a net unipolar charge. However, the back corona current fraction approaches 1 as the resistivity of the dust cake increases. The degradation of precipitator performance by back corona can be managed if the dust resistivity can be controlled.

Resistivity can be controlled by adding chemicals to the gas that adsorb on the particles and change their characteristics. Sulfuric acid, in concentrations of a few μL/L, is effective for this purpose. Sodium carbonate is used in some high temperature precipitators where the particle resistivity is affected by the internal depletion of sodium ions. Ammonia can prevent back corona but appears to affect the gas properties more than the dust cake resistivity.

Another way to prevent back corona is to pulse the corona intermittently. The dust layer breakdown is a function of the time-averaged current density which can be reduced by as much as a factor of 10 by intermittent energization. The peak electric field remains unchanged or may increase slightly during pulsing, while the time-averaged electric field is somewhat reduced. Particle charging responds primarily to the peak electric field, while particle collection is most affected by the average electric field. Pulsing can, therefore, control back corona onset quite well over about a decade of resistivity and offer some improvement over a broader range.

Low-Voltage Sparking. Sparking at lower than expected voltages reduces the performance of the precipitator in proportion to the voltage reduction. Back corona does cause low-voltage sparking over a rather narrow range of resistivities, but the correction is to control the back corona. Other more likely causes of low voltage sparking are misalignment of electrodes and insulator problems.

Electrode misalignment brings some part of the high voltage system too close to the grounded plate system. As a result, the electric field (roughly voltage/distance) becomes high enough to cause sparking. Such sparking is usually at the same spot and may cause noticeable electrode erosion. Until the misalignment is corrected, the voltage can never be raised to its normal value.

Insulators perform the unobserved, but necessary function of supporting the discharge electrodes without conducting electricity. When insulators become contaminated, repeated sparking along an insulator can erode the surface or carbonize materials on the surface to the point that cleaning is insufficient to restore proper operation. Condensation of moisture or acid on the insulators during a startup is another source of insulator contamination. Heated air purges are used to prevent such condensation.

ADVANCED TOPICS IN PRECIPITATION

Electrostatic precipitation is a mature technology, much like the automobile. Although we do not expect to find major technological advances in precipitators, the variety of applications and pressure of external regulations will bring about slow, continuous improvements in precipitator operations. Improvements are often measured in terms of capital and operating cost reductions or increased reliability because precipitator technology seems capable of controlling particle emissions to any desired level, given a large enough machine. Some of the areas that could prove fruitful in these directions are discussed below.

Rapping Loss Reduction

Reduction of rapping losses has potential for improving the collection performance of existing precipitators and reducing the size of new precipitators. Moreover, the particles in the emitted dust from rapping have a substantial portion below 10 μm in diameter, a region on which future environmental regulations may focus. Elimination of rapping emissions would improve conformance to such regulations. A better understanding of rapping emissions would improve chances for control in existing precipitators. The following areas are suggested points of investigation.

Cohesion. The cohesion of the dust cake affects that manner in which it falls when rapped. Is it possible to determine values of cohesivity acceptable for rapping? How does the layer thickness affect the rapping properties, and are there optimum values?

Size Distribution. In many cases, the rapping emissions have an almost universal size distribution with a mean diameter of 6 to 10 μm. In others, the rapping distribution is similar to the size distribution of the particles being collected. What are the factors that govern the rapping size distribution? Can the size distribution be predicted from particle properties?

Mechanical Design. The rapping reentrainment model suggests that mechanical dimensions (electrode spacing, length, and height of collection plate) affect the amount of material reentrained. Do these factors play the role that the rapping reentrainment model implies? Are there ways to vary the electrode spacing that would reduce rapping emissions?

Flow Control. The rapping model suggests that the gas velocity near the collecting plate is critical for controlling rapping emissions. Innovative suggestions have been made that the normal uniform gas velocity distribution could be made beneficially nonuniform, with rapping emissions the target of the change. Is this feasible? Plate stiffeners designed to shield the dust cake from the gas flow have been made. Do they perform as designed?

Conditioning Agents

Gas conditioning agents have been long used to improve the operation of precipitators. Water is one of the simplest conditioning agents. Addition of water droplets to a hot gas cools and humidifies the gas. The lower gas volume increases treatment time in the precipitator, while the humidity reduces the dust resistivity for some particles. Sulfuric acid (or SO_3) is an agent designed to modify the resistivity of the particles for back corona control. Ammonia is an agent that has been used to suppress back corona and improve the cohesivity of the dust cake; its back corona action is not certain but may result from the formation of a fine particle mode that increases the space charge. Sodium conditioning to improve the resistivity of dust cakes is another type of conditioning.

Although conditioning agents target specific precipitator problems, they do not always perform as intended. Some flyash compositions are not responsive to sulfuric acid conditioning, for example, or the precipitator operating temperature may be inappropriate. Understanding the methods by which each agent improves precipitator operation would guide the best use of the agent and could lead to development of new conditioning agents for both the standard problems and new problem areas.

Back Corona Identification and Characterization

Although many cases of back corona are obvious from V–I curves and the poor performance of the precipitator, back corona may occur marginally in portions of the precipitator without being detected. Precipitator performance may suffer as a result. If a better means of detecting back corona were available, such problems could be identified and corrected. Alternatively, if a conditioning agent is being added to the flue gas for resistivity control, back corona detection could be used to optimize the amount of agent introduced. With present methods of operation, the injection of conditioning agents is usually made to control the resistivity under worst-case conditions. Small changes in flyash composition may shift the resistivity enough that conditioning might not even be required.

Ash resistivity can be very sensitive to temperature; temperature differences across the face of the precipitator have been known to put part of the precipitator into back corona, while the remainder works quite well. Direct detection of back corona would be useful in finding the causes that contribute to it.

Despite the obvious degradation that back corona causes, it has proven difficult to make quantitative predictions of its severity. Based on the performance of precipitators with measured dust resistivities, the trends of performance can be estimated but not predicted. One technique that has been used is to correlate performance with a "useful" current density, the current density available to charge particles before back corona sets in. This technique approximates the degradation of performance but does not provide insight into the actual mechanisms of degradation.

Based on the physics of gas discharges, back corona onset should be affected by the thickness of the dust layer. This means that the removal of the dust by rapping should change the back corona characteristics. This effect has not been studied, but it might well alter the rapping strategy in a precipitator with back corona.

Improved Corona Electrodes

Most corona electrodes operate similarly above corona onset; the nature of the corona almost guarantees it. The design of a corona electrode can control the corona onset voltage, however, and limit the corona to specific zones along the length of the electrode. These controllable properties may be put to use in cases where high concentrations of particles produce space charge problems or put heavy loads on the collection plates. With new electrode designs, it should be possible to distribute the charging and collecting of particles over more of the precipitator sections, reducing the impact of the high concentrations.

Improved Collection of Submicron Particles

Precipitators have a minimum in collection performance below 1 μm diameter, at the point where the particle charge is decreasing, and the Cunningham slip factor is still close to 1. This size range, however, contains particles that are most respirable and are most subject to future environmental regulation. Improvement of particle collection in this size range will require improvements to particle charging and maintenance of high electric fields. Losses from sneakage and rapping reentrainment are relatively insignificant for these particles.

Particle Formation in Precipitators and other Control Devices

Experimental measurements in operating precipitators below 1 μm diameter have shown that particles condense from the gas phase and grow to measurable sizes *within* the precipitator. These particles may be present at the outlet at higher concentrations than at the inlet. Such growth has been observed when, for example, sulfuric acid gas condenses into a particle phase as the temperature is lowered. The precipitator is hindered in collecting these particles because they pass through most of the machine as a gas. Understanding the concentrations of materials and the temperature profiles that lead to this phenomenon will be most important in preventing or controlling the emission of such particles, especially since the most toxic metals often condense preferentially on such small particles.

Adaptive Computer Controls

Large precipitators often run at full power even though the boiler may only be at partial output. This practice wastes power and may even raise emissions because the temperature and resistivity of the precipitator and ash are controlled by the amount of gas passing through. The computer models of precipitators are accurate enough to predict many of these effects in real time and could be put to use optimizing precipitator operation for changing load conditions (see PREDICTIVE CONTROL). Using real time inputs of boiler and precipitator parameters, such computer control could permit power reductions under reduced load conditions, while keeping the emissions low. An approach such as this might be used to offset increased precipitator size (for better performance at full load) with savings in operating costs.

BIBLIOGRAPHY

1. S. A. Self and M. Mitchener, *Basic Studies to Reduce Electrostatic Precipitator Size and Cost,* EPRI Report CS-3226, Palo Alto: Electric Power Research Institute, 1983.
2. H. J. White, *Industrial Electrostatic Precipitation,* Reading, MA: Addison-Wesley, 1963.
3. J. H. Turner, P. A. Lawless, T. Yamamoto, D. W. Coy, G. P. Greiner, J. D. McKenna, and W. M. Vatavuk, Electrostatic precipitators, In A. J. Buonicore and W. T. Davis (eds.), *Air Pollution Engineering Manual,* New York: Van Nostrand Reinhold, 89–113, 1992.
4. S. Matts and P. Ohnfeldt, Efficient gas cleaning with SF electrostatic precipitators, Fläkt, 1–12. This was a private company publication. See White, p. 62, for discussion.
5. P. A. Lawless and L. E. Sparks, A review of mathematical models for ESPs and comparison of their successes. In S. Masuda (ed.), *Proceedings: Second International Conference on Electrostatic Precipitation,* Kyoto, Pittsburgh: Air Pollution Control Assoc., 513–522, 1984.
6. H. E. Rose and A. J. Wood, *An Introduction to Electrostatic Precipitation in Theory and Practice,* London: Constable and Company, 1966.
7. J. Katz, *The Art of Electrostatic Precipitation,* Munhall, PA: Precipitator Technology, Inc., 1979.
8. J. B. Loeb, *Electrical Coronas—their Basic Physical Mechanisms,* Berkeley and Los Angeles: University of CA Press, 1965.
9. S. Oglesby Jr. and G. B. Nichols, *Electrostatic Precipitation,* New York: Marcell Dekker, 1978.
10. F. W. Peek, *Dielectric Phenomena in High-Voltage Engineering,* New York: McGraw-Hill, 1929.
11. P. A. Lawless, K. J. McLean, L. E. Sparks, and G. H. Ramsey, Negative corona in wire-plate electrostatic precipitators. Part I:

characteristics of individual tuft-corona discharges. *J. Electrostatics* **18**, 199–217, 1986.

12. K. J. McLean, P. A. Lawless, L. E. Sparks, and G. H. Ramsey, Negative corona in wire-plate electrostatic precipitators. Part II: calculation of electrical characteristics of contaminated discharge electrodes, *J. Electrostatics,* **18**: 219–231, 1986.
13. R. S. Sigmond, Simple approximate treatment of unipolar space-charge-dominated coronas: the Warburg law and the saturation current, *J. Applied Physics,* **53**: 891–898, 1982.
14. C. T. Phelps and R. F. Griffiths, Dependence of positive streamer propagation on air pressure and water vapor content, *J. Appl. Physics,* **47**: 2929–2934, 1976.
15. P. A. Lawless and L. E. Sparks, Measurement of ion mobilities in air and sulfur dioxide-air mixtures as a function of temperature, *Atm. Env.,* **14**: 481–483, 1980.
16. P. A. Lawless, Unpublished data, 1993.
17. P. A. Lawless and T. Yamamoto, Improving ESP performance by reducing losses, In M. Rea (ed.), *Proceedings: Third International Conference on Electrostatic Precipitation,* Abano-Padova, 433–442, 1987.
18. P. C. Reist, *Introduction to Aerosol Science,* New York: Macmillan, 1984.
19. R. A. Fjeld and A. R. McFarland, Evaluation of select approximations for calculating particle charging rates in the continuum regime, *Aerosol Sci. Tech.,* **10**: 535–549, 1988.
20. J. D. Klett, Ion transport to cloud droplets by diffusion and conduction, and the resulting droplet charge distribution, *J. Atmos. Sci.,* **28**: 78–85, 1971.
21. P. A. Lawless, Particle charging bounds, symmetry relations, and an analytic charging rate model for the continuum regime, *J. Aerosol Sci.,* **2**: 191–215, 1996.
22. D. K. Hutchins, M. H. Harper, and R. L. Felder, Slip correction measurements for solid spherical particles by modulated dynamic light scattering, *J. Aerosol Sci.,* **22**: 202–218, 1996.
23. P. A. Lawless, Modeling of electrostatic precipitator charging, collection, and rapping reentrainment, Poster Session: 10th particulate Control Symposium and 5th International Conference on Electrostatic Precipitation, Washington, 1983.
24. S. A. Self, G. B. Moslehi, M. Mitchener, and R. Leach, Electromechanics and reentrainment of precipitated ash. In Harry J. White (ed.) *Proc. Int. Conf. on Electrostatic Precipitation,* 399–440, 1981.

Reading List

The classical reference for precipitators is the out-of-print book by Harry White (2). This book has been reprinted by the International Society on Electrostatic Precipitation and can be obtained from: Dr. Robert Crynack, ISESP c/o Wheelabrator APC, 441 Smithfield Street, Pittsburgh, PA 15222-2292.

The next best general reference is the book by Oglesby and Nichols (9).

A promising new book on the subject is: K. R. Parker, ed., *Applied Electrostatic Precipitation,* London: Blackie Academic and Professional, 1997.

A comprehensive operating/maintenance discussion of precipitators is the book by Katz, (7).

For a Detailed Look at Corona Processes:

L. B. Loeb, *Basic Processes of Gaseous Electronics,* Berkeley and Los Angeles: University of CA Press, 1961, or (8).

Others

Industrial Gas Cleaning Institute, Inc. *Terminology for Electrostatic Precipitators,* EP-1, 1984.

Phil A. Lawless
Research Triangle Institute
Ralph F. Altman
Electric Power Research Institute